Laser Modification of Ultracold Atomic Collisions: Theory

Paul S. Julienne and Robert Heather
Molecular Physics Division, National Institute of Standards and Technology, Gaithersburg, Maryland 20899
(Received 26 June 1991)

Specific molecular mechanisms are proposed for associative ionization collisions of ultracold sodium atoms in a hybrid optical trap. When an intense, strongly detuned optical trap laser is on, the ionization rate is modulated by molecular bound-state resonances which are strongly affected by field dressing. When the weak, slightly detuned optical molasses lasers are on to provide cooling, an excitation mechanism which produces the two excited atoms at large internuclear separation in different hyperfine states accounts for the lower observed ionization rate.

PACS numbers: 34.50.Fa, 32.80.Pj, 34.50.Rk

The associative ionization (AI) of two excited Na atoms to make a Na_2^+ molecule has been studied at normal [1] and ultracold temperatures [2]. The following Letter by Lett *et al.* [3] reexamines submillikelvin collisions by time resolving the AI signal in the trapping and molasses phases of their hybrid laser trap. Although the new experiment verifies the qualitative prediction [4] that the ultracold ionization rate coefficient should be modified by laser excitation conditions so that it is much smaller in the optical molasses phase than in the trapping phase, the ion signal in molasses is much larger than expected, and the ion signal in the trapping phase shows clear evidence of molecular structure in its dependence on trap-laser detuning. In the conventional view of AI the two approaching Na atoms are excited by laser photons as free, independent atoms while they are still very far apart, which then collide along a potential curve of a doubly excited state of the Na_2 molecule, ultimately ejecting an electron when the two atoms reach an internuclear separation R comparable to the equilibrium internuclear separation R_e of the Na_2^+ molecular ion. By contrast, the long-time scale of an ultracold collision, which may be several excited-state lifetimes [5–8] only permits the ionization event near R_e to occur if the slowly approaching atoms are excited to the doubly excited potential curve while they are close enough together that they can move to R_e without decaying by spontaneous emission. This excitation and survival process is a sequential molecular process which is strongly dependent on laser detuning and intensity and operates in a fundamentally different way during the trapping and molasses phases of the NIST hybrid trap. We propose here specific molecular mechanisms that explain the new data and illustrate the unique sensitivity of ultracold collisions to laser manipulation.

Figure 1 schematically illustrates the following sequential molecular pathway for AI:

$$\begin{aligned} \mathrm{Na}+\mathrm{Na}+2\hbar\omega &\rightarrow \mathrm{Na_2}^*(P_{3/2}+S)+\hbar\omega \\ &\rightarrow \mathrm{Na_2}^{**}(P_{3/2}+P_{3/2}) \\ &\rightarrow \mathrm{Na_2}^+ + e^- , \end{aligned} \tag{1}$$

where the parentheses give the asymptotic atomic states with which the molecular states correlate. The excitations occur in the long-range molecular region near Condon points, where the photon energy $\hbar\omega$ matches the difference between upper and lower molecular potentials. We will first identify the important molecular potentials, and then describe numerical models which allow us to estimate the effective rate coefficients in the molasses and trap phases. Several papers have shown that the conventional scattering viewpoint must be modified for low-temperature collisions [5–8]. Effective rate coefficients can be defined for AI [7,8], just as they have been for trap loss collisions due to a change of fine-structure state [6,7], namely,

$$d(\mathrm{ions})/dt = K_{\mathrm{eff}} NN = K_{\mathrm{eff}}^{**} N^* N^* , \tag{2}$$

where N and N^* are the respective ground- and excited-state densities, and N^* is measured by the fluorescence rate. Here we will calculate K_{eff} referenced to the ground-state density [9].

Researchers at Orsay have calculated Na_2 diabatic molecular potentials for $R < 10a_0$ and have identified a $^3\Sigma_u^+$ state as the likely Na_2^{**} state which leads to AI at

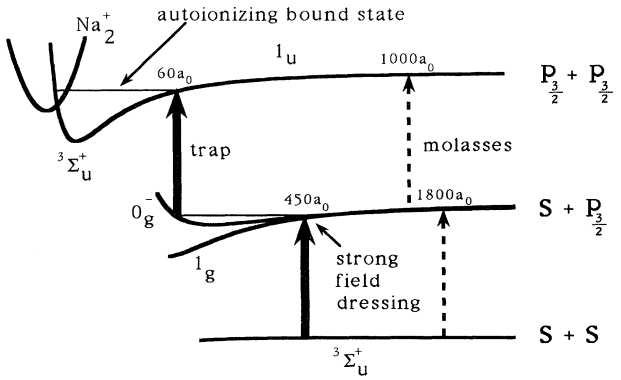

FIG. 1. Schematic diagram of AI mechanisms. The molecular-state symmetries are indicated, as well as the approximate R (in units of $a_0 = 0.529 \times 10^{-8}$ cm) of the Condon points for the trap (solid) and molasses (dashed) detunings.

normal temperatures [10]. A $^1\Delta_g$ state may also make some contribution, but no other states are likely to provide important entrance channels. When R is large the quadrupole-quadrupole interaction between two $^2P_{3/2}$ atoms gives rise to potentials which vary as C_5/R^5 and can be attractive or repulsive. Approximate Na_2^{**} molecular potentials in the range $(18-40)a_0$ have recently been calculated [11], using effective core potential methods with full two-electron configuration interaction [12]. Although these potentials allow us to give a qualitative assessment of AI, accurate long-range potentials are still needed for more quantitative studies. Upon diagonalizing the electronic plus spin-orbit Hamiltonian, we find that the only asymptotic attractive states from $P_{3/2}+P_{3/2}$ have 1_u, 2_u, and 1_g symmetry (the number gives the angular momentum projection on the internuclear axis), but the latter two connect at short range with repulsive states that do not undergo AI. Therefore, only the 1_u Na_2^{**} entrance channel is likely to contribute as $T\rightarrow 0$. The attractive 1_u state from $P_{3/2}+P_{3/2}$ correlates with the 1_u component of an attractive $^3\Sigma_u^+$ short-range state through an avoided crossing near $20a_0$. We make the reasonable assumption that this $^3\Sigma_u^+$ state just inside the crossing connects with the diabatic $^3\Sigma_u^+$ state calculated by Dulieu, Giusti-Suzor, and Masnou-Seeuws [10] for $R<10a_0$. Using close-coupling scattering calculations with the approximate potentials of Ref. [11], we calculate at normal temperatures a single-pass probability $P_x\approx 1$ for traversing this crossing from 1_u to $^3\Sigma_u^+$. This probability is reduced to $P_x=0.3$ as $T\rightarrow 0$, a result consistent with the Landau-Zener curve-crossing formula, and implying a velocity-dependent P_x as T is lowered from higher T. The high-temperature average probability of AI, given unit flux on the $^3\Sigma_u^+$ state, can be calculated from the measured cross section if we know the maximum partial wave that contributes, given by the maximum residual rotational state of the product molecular ion (the electron carries off very little angular momentum). Given the experimental uncertainty in the high-temperature rate coefficient near 0.05-eV collision energy [1] this probability lies in the range 0.2–0.5, where the smaller value is consistent with the multichannel-quantum-defect-theory calculation of Ref. [6] and the isotropic cross section of Meijer [1]. Reducing this by P_x as $T\rightarrow 0$ gives an AI probability of ≈ 0.1, given unit flux on the long-range Na_2^{**} 1_u state.

The only attractive intermediate Na_2^* molecular states with dipole-allowed transitions to the 1_u AI entrance-channel state are the attractive 0_g^- and 1_g states. These have long-range potentials varying as $-C_3/R^3$ (neglecting retardation corrections), with respective values [13] of C_3 of 6.48 and 10.0 times $e^2a_0^2$ and respective decay rates [14] of 2 and 1.21 times the atomic decay rate $\tau_A^{-1}=\frac{1}{16}\times 10^{-9}$ s. The strongly attractive 1_g state connects at short range with the chemically bound $^1\Pi_g$ state, whereas the 0_g^- state is a long-range state [15] bound by only about ≈ 50 GHz and with an *inner* turning point near $60a_0$. These Na_2^* states have a much longer range of interaction than either the Na+Na or Na_2^{**} states and control the molecular detuning and the location of the Condon points, which determine where the Na_2^{**} 1_u state can be excited in an ultracold collision. Dipole-allowed transitions to these g intermediate states are only possible from the ground $^3\Sigma_u^+$ state.

In the optical molasses phase of the hybrid trap [2,3], cooling is provided by six molasses beams having total power of 50 mW/cm^2 and detuned about 1 natural linewidth, $\Gamma/2\pi=0.010$ GHz, to the red of the $^2S(F=2)\rightarrow {}^2P_{3/2}(F=3)$ transition. The on-resonance Rabi frequency is comparable to Γ, and the thermal energy in the trap, k_BT, is comparable to $\hbar\Gamma$. The Condon points for the Na+Na$\rightarrow Na_2^*$ transition are near $R=1700a_0$ and $1900a_0$ for the 0_g^- and 1_g states, respectively, schematically shown in Fig. 1. But the $Na_2^*\rightarrow Na_2^{**}$ $S(F=2)\rightarrow P(F=3)$ transition never comes into resonance at long range because of the strong blue detuning introduced by the intermediate potential. However, the other hyperfine transition, $S(F=2)\rightarrow P(F=2)$, is blue detuned relative to the molasses laser because the $P(F=2)$ level is 0.060 GHz *below* the $P(F=3)$ level. Thus, the blue detuning introduced by the Na_2^* intermediate states brings this $Na_2^*\rightarrow Na_2^{**}$ hyperfine transition into resonance at Condon points of $R=950a_0$ and $1100a_0$ for the respective 0_g^- and 1_g intermediate states.

The effective rate coefficient $K_{\rm eff}$ can be calculated using the weak-field quasistatic excitation model of Gallagher and Pritchard [6], as modified by Julienne and Vigué to include the role of relative angular momentum ("partial wave" l) [7], once we have generalized it to include a second excitation step. (Gallagher [8] has also proposed such a generalization which interprets ultracold AI by mechanisms very different from the ones described here.) We calculate that the AI rate due to the $Na_2^*\rightarrow Na_2^{**}$ on-resonance process $(F=2\rightarrow F=2)$ dominates that for the off-resonance process $(F=2\rightarrow F=3)$. The calculated rate expression includes the excitation of the Na_2^* state over a range of R near the Condon point, propagation with flux loss due to Na_2^* decay between the point of excitation and the second Condon point, where the transition to Na_2^{**} occurs, followed by similar propagation to small R where AI occurs according to the probability 0.1 deduced above for the 1_u state as $T\rightarrow 0$. The effective rate coefficient is reduced for molasses excitation conditions because excited-state radiative decay during the collision reduces the scattering flux, since the time required to move from the Condon points to R_e is longer than the excited-state lifetimes. Our calculation for the conditions of the experiment find $k_{\rm AI}=8\times 10^{-14}$ cm^3/s, which is in good agreement with the measured value [3], $4.3^{+5.5}_{-2.6}\times 10^{-14}$ cm^3/s.

Laser excitation conditions are extremely different during the trapping phase, for which an intense, tightly fo-

cused laser provides a dipole-force optical trap. The trap-laser detuning $\Delta/2\pi$ was varied from about -0.6 to -5 GHz, or 60 to 500 natural widths to the red of resonance. The on-resonance Rabi frequency $\Omega/2\pi$ was about 1 GHz, or 100 natural widths. The intense circularly polarized laser optically pumps the atoms to the ground "stretched state" with $F=2$, $M_F=2$. This forces collisions to occur on the ground $^3\Sigma_u^+$ state, from which excitation can occur to the same 0_g^- or 1_g intermediate states as for AI in molasses; however, there are very important differences. The strong detuning leads to excitation of the Na_2^* states at much smaller R, $410a_0$ and $480a_0$, respectively, for 0_g^- and 1_g at -0.6-GHz detuning and half these distances at -5-GHz detuning. For such detunings the vibrational spacing [11] of these Na_2^* states is much larger than the natural width but much smaller than the on-resonance Rabi frequency. Therefore, molecular bound-state resonance structure, strongly perturbed by the intense radiation field, modulates the AI rate. Negligible spontaneous emission occurs during a molecular vibration, which can bring the atoms to the inner turning point near $60a_0$, where absorption can occur with good Franck-Condon factors to an autoionizing bound molecular level of the Na_2^{**} 1_u state.

In contrast to our model for AI in the molasses phase, our theoretical model of collisions during the trapping phase uses only a conservative Hamiltonian which neglects excited-state emission. This is permissible since the collision should be viewed as that of two field-dressed atoms [4] in their "ground" state, that is, the one which correlates with two S atoms when the field is turned off. The primary role of spontaneous emission when R is large is to establish the populations [16] of the quasimolecular dressed states in a radiative cascade. For the large detunings in the trap this insures that almost all the population is in the ground dressed state, which should therefore be viewed as the entrance channel of scattering theory which is nearly unaffected by spontaneous emission. Excitation from this channel occurs when the atoms are close enough together that they do not decay, that is, the vibrational spacing and the widths of the excited bound levels due to stimulated emission or autoionization are all larger than the spontaneous decay width.

Our theoretical calculation of the trap-phase K_{eff} is a standard close-coupled calculation for a collision in an intense radiation field [17]. The model includes the following features: (1) The known long-range potentials and transition dipoles are used for the ground $^3\Sigma_u^+$ entrance channel, the first excited 0_g^- and 1_g states, and the doubly excited 1_u state. Competing predissociation broadening of the bound levels of the 0_g^- and 1_g states does not occur, since these states will not decay to $S+P_{1/2}$ with a change of fine-structure level during the collision [7]. (2) Autoionization of the 1_u AI channel is simulated by introducing an extra "artificial" channel with adjustable coupling which effectively acts as an optical potential to simulate AI in the region near R_e and gives adjustable autoionization widths to the Na_2^{**} bound molecular levels. Since the model does not include predissociation decay channels of these autoionizing bound levels, the calculated AI rate is an upper bound to the true rate, which will be reduced by processes left out of the model. (3) The coupled-channel expansion uses a total angular momentum basis $|JM\rangle$, allowing for $\Delta J=0,\pm 1$ molecular transitions from an entrance-channel state of even l only, due to homonuclear symmetry considerations for stretched state collisions. Averaging over all directions of the collision axis relative to the polarization vector of the laser is done using a predynamically averaged Rabi frequency, reduced by $1/\sqrt{3}$ from its maximum value [17]. One consequence of our calculation is that field dressing mixes in excited-state attractive $1/R^3$ character in the long-range ground entrance-channel potential [4], thereby reducing centrifugal barriers and allowing extra partial waves to contribute to K_{eff}.

Figure 2 shows the results of our calculation of the trap-phase K_{eff} versus trap-laser detuning for a single collision energy, $E/k_B=0.75$ mK, and with a Rabi frequency of 1.5 GHz for the atomic transition. The figure clearly shows the existence of complex resonance structure in the AI spectrum. Broadening due to the spread in collision energy is negligible, since k_BT is so small, ≈ 0.01 GHz. The 0_g^- and 1_g intermediate states both have bound states which are mixed and interfere in a complex way due to the strong perturbing effect of the intense laser field, for which the Rabi frequency is larger than the vibrational frequency. The AI rate is large when both Na_2^* and Na_2^{**} resonances can be excited at the same detuning. However, our interpretation of these multichannel resonances is beyond the scope of this brief

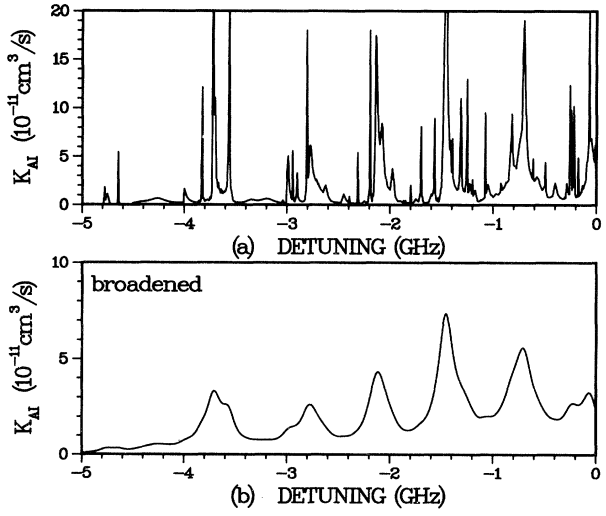

FIG. 2. (a) Calculated effective AI rate coefficient vs trap-laser detuning for an atomic on-resonance Rabi frequency of $\Omega/2\pi=1.5$ GHz. (b) Same as (a) convolved with a Lorentzian of width 0.15 GHz to simulate inhomogeneous broadening by averaging over all molecular Rabi frequencies.

Letter. Since the correct procedure would be to introduce all Rabi frequencies for the individual projection quantum numbers M in the rotational basis $|JM\rangle$, instead of using a spherically averaged Rabi matrix element to simulate averaging over all directions of collision axis relative to polarization vector, we have also summed in selected regions of the spectrum the calculated contributions from individual M states and compared to the model with the averaged matrix element. Because of the spread in light shifts, this results in an inhomogeneously broadened spectrum. Our tests indicate that this broadening and that due to unresolved hyperfine structure can be simulated by convolving the spectrum in Fig. 2(a) with a Lorentzian with a width of 0.15 GHz. The result in Fig. 2(b) shows features qualitatively similar to the experimental spectrum [3]. The structure in Fig. 2(b) which survives the convolution is related to the vibrational spacing in the intermediate Na_2^* state and the rotational spacing of a single vibrational level of the Na_2^{**} state; the cutoff in K_{eff} below $\Delta \approx -4.5$ GHz is due to reaching the position of the $J=0$ level of this autoionizing bound state. However, there are too many uncertainties and adjustable parameters in the model to attempt a quantitative comparison with the data. Using our calculated rate coefficient for molasses and our upper bound to the rate coefficient in the trap (see Fig. 2), we now predict an upper bound of about 400 for the ratio of rate coefficients in the trap and molasses phases of the experiment. This is consistent with the observed [3] range of this ratio, 20 to 200 with an average value of 60. Our two distinct models of AI for the very different laser excitation conditions in the molasses and trap phases of the NIST experiment illustrate the unique sensitivity of ultracold-collision rate coefficients to modification by excited-state decay and external fields. Additional experimental and theoretical development is needed to understand better the dependence of these novel collisions on laser intensity and detuning and to interpret the bound-state structure near the $P+P$ asymptote. Two-color experiments could be very useful by allowing more control over the excitation and survival process [3,8].

The authors thank M. Krauss for providing his unpublished potentials, J. Dalibard for helpful comments, and the Office of Naval Research for partial support.

[1] J. Weiner, A. Giusti-Suzor, and F. Masnou-Seeuws, Adv. At. Mol. Opt. Phys. **26**, 209 (1989); H. A. J. Meijer, Z. Phys. D **17**, 257 (1990), and references therein.

[2] P. L. Gould, P. D. Lett, P. S. Julienne, W. D. Phillips, H. R. Thorsheim, and J. Weiner, Phys. Rev. Lett. **60**, 788 (1988).

[3] P. D. Lett, P. S. Jessen, W. D. Phillips, S. L. Rolston, C. I. Westbrook, and P. L. Gould, following Letter, Phys. Rev. Lett. **67**, 2139 (1991).

[4] P. S. Julienne, Phys. Rev. Lett. **61**, 698 (1988).

[5] P. S. Julienne and F. Mies, J. Opt. Soc. Am. B **6**, 2257 (1989).

[6] A. Gallagher and D. Pritchard, Phys. Rev. Lett. **63**, 957 (1989).

[7] P. S. Julienne, R. Heather, and J. Vigué, in *Spectral Line Shapes,* edited by L. Frommhold and J. W. Keto, AIP Conference Proceedings No. 216 (American Institute of Physics, New York, 1990), Vol. 6, p. 191; P. S. Julienne and J. Vigué, Phys. Rev. A **44**, 4464 (1991).

[8] A. Gallagher, Phys. Rev. A **44**, 4249 (1991).

[9] This definition includes a homonuclear symmetry factor of $\frac{1}{2}$ in the definition of k_{AI}, whereas the definition of Meijer [1] puts this factor with the density, $N^2/2$. Rate coefficients defined according to Meijer are twice as large as defined here.

[10] A. Henriet, O. Dulieu, and F. Masnou-Seeuws, Z. Phys. D **18**, 287 (1991); O. Dulieu, A. Giusti-Suzor, and F. Masnou-Seeuws, J. Phys. B (to be published).

[11] M. Krauss (private communication).

[12] M. Krauss and W. Stevens, J. Chem. Phys. **93**, 4236 (1990).

[13] B. Bussery and A. Aubert-Frecon, J. Chem. Phys. **82**, 3224 (1985).

[14] M. Movre and G. Pichler, J. Phys. B **13**, 697 (1980).

[15] W. C. Stwalley, Y.-H. Uang, and G. Pichler, Phys. Rev. Lett. **41**, 1164 (1978).

[16] J. Dalibard and C. Cohen-Tannoudji, J. Opt. Soc. Am. B **2**, 1707 (1985).

[17] P. L. DeVries and T. F. George, Mol. Phys. **36**, 151 (1978); **38**, 561 (1979); Phys. Rev. A **18**, 1751 (1978); P. S. Julienne and F. H. Mies, Phys. Rev. A **25**, 3399 (1982); J. C. Peploski and L. Eno, J. Chem. Phys. **89**, 3579 (1988).